structural interaction. There are several possible candidates for the stop signal: the polar side chains of Ser or Asp might present competing H-bonding sites for the N—H···O=C donor–acceptor pairs of the α-helix backbone. This has been hypothesized as an important contribution for terminating helices early in the folding process (Presta & Rose, 1988). Alternatively, the involvement of two side chains in a specific interaction might prevent the elongation of the helix. In fact, it has recently been observed that a salt bridge between Glu-2 and Arg-10 in a peptide analogue of the first 13 residues of RNase A terminates the N-terminal end of the helix between Glu-2 and Thr-3 (John J. Osterhout, personal communication). These are only two of several possible interactions which might terminate helices. If these interactions are stabilized by TFE in concert with α-helix stabilization, the stop signal would be expected to remain intact in the presence of TFE.

ACKNOWLEDGMENTS

We thank Drs. Robert L. Baldwin and Peter S. Kim for providing the S-peptide samples and for many valuable discussions. The Brüker AM-500 NMR spectrometer at the Institute for Cancer Research in Philadelphia is supported by Instrument Grants RR 02497 (NIH) and DMB 84-13986 (NSF), by an award from Marie Z. Cole Montrose, by NIH Grants CA 06927 and RR 05539, and by an appropriation from the Commonwealth of Pennsylvania awarded to the Institute for Cancer Research. The Brüker AM-400 NMR spectrometer in the College of Basic Sciences at Louisiana State University was funded in part by NIH Shared Instrumentation Grant RR 02459.

Registry No. S-Peptide, 65742-22-5.

REFERENCES

Bodenhausen, G., Kogler, H., & Ernst, R. R. (1984) *J. Magn. Reson. 58*, 370–388.
Brown, J. E., & Klee, W. A. (1971) *Biochemistry 10*, 470–476.
Filippi, B., Borin, G., & Marchiori, F. (1976) *J. Mol. Biol. 106*, 315–324.
Filippi, B., Borin, G., Moretto, V., & Marchiori, F. (1978) *Biopolymers 17*, 2545–2559.
Kim, P. S., & Baldwin, R. L. (1984) *Nature 307*, 329–334.
Marion, D., & Wüthrich, K. (1983) *Biochem. Biophys. Res. Commun. 113*, 967–974.
Nelson, J. W., & Kallenbach, N. R. (1986) *Proteins 1*, 211–217.
Presta, L. G., & Rose, G. D. (1988) *Science 240*, 1632–1641.
Rance, M., Sørensen, O. W., Bodenhausen, G., Wagner, G., Ernst, R. R., & Wüthrich, K. (1983) *Biochem. Biophys. Res. Commun. 117*, 479–485.
Rico, M., Santoro, J., Bermejo, F. J., Herranz, J., Nieto, J. L., Gallego, E., & Jiménez, M. A. (1986) *Biopolymers 25*, 1031–1053.
Shoemaker, K. R., Kim, P. S., Brems, D. N., Marqusee, S., York, E. J., Chaiken, I. M., Stewart, J. M., & Baldwin, R. L. (1985) *Proc. Natl. Acad. Sci. U.S.A. 82*, 2349–2353.
Shoemaker, K. R., Kim, P. S., York, E. J., Stewart, J. M., & Baldwin, R. L. (1987) *Nature 326*, 563–567.
Sueki, M., Lee, S., Powers, S. P., Denton, J. B., Konishi, Y., & Scheraga, H. A. (1984) *Macromolecules 17*, 148–155.
Wagner, G. (1983) *J. Magn. Reson. 55*, 151–156.
Wider, G., Hosur, R. V., & Wüthrich, K. (1983) *J. Magn. Reson. 52*, 130–135.
Zimm, B. H., & Bragg, W. K. (1959) *J. Chem. Phys. 31*, 526–535.

^{1}H NMR Characterization of *Chromatium gracile* High-Potential Iron Protein and Its Ruthenium-Modified Derivatives. Modulation of the Reduction Potentials in Low- and High-Potential [Fe_4S_4] Ferredoxins†

M. Sola,‡ J. A. Cowan, and Harry B. Gray*
Arthur Amos Noyes Laboratory, California Institute of Technology, Pasadena, California 91125
Received October 19, 1988; Revised Manuscript Received February 17, 1989

ABSTRACT: The NMR spectra of the high-potential iron protein from the photosynthetic bacterium *Chromatium gracile* and its ruthenium-labeled (His-42 and His-20) derivatives are reported. The isotropically shifted resonances in both the oxidized and reduced forms show a complex pH dependence due to the presence of three ionizable residues (Glu-44, His-20, and His-42). Assignments have been made to specific residues and the spectral features compared to those of other bacterial HiPIP's. The decrease in the reduction potential with increasing pH for this class of proteins is attributed to stabilization of the oxidized state of the cluster by delocalization of electron density onto the neighboring Tyr-19 residue.

High-potential iron proteins (HiPIP's) are a class of enzymes containing [Fe_4S_4] clusters that possess large positive reduction potentials ($E°$ ranging from 100 to 350 mV) and are frequently found in photosynthetic bacteria, although one example has also been associated with a denitrifying bacterium (Palmer, 1975; Carter, 1977; Bartsch, 1978; Meyer et al., 1983). An electron-transport role has commonly been assumed, although there has been no conclusive evidence to support this belief. A related series of [Fe_4S_4] ferredoxins (Fd's) that contain a structurally identical prosthetic group differ in the cluster reduction potential, typically $E° \sim -400$ mV, and have led to much discussion concerning the factors

† Contribution No. 7872. This research was supported by the National Institutes of Health (DK-19038). J.A.C. thanks the Science and Engineering Research Council (United Kingdom) for a NATO Postdoctoral Fellowship.
‡ Present address: Department of Chemistry, University of Modena, Via Campi 183, 41100 Modena, Italy.

0006-2960/89/0428-5261$01.50/0

Table I: ^{1}H NMR Parameters of the Reduced Form of Native HiPIP from *C. gracile* and Its Ru(III) Derivatives[a]

ppm^N	ppm^{42}	ppm^{20}	ppm^V	T_1N	T_1^{42}	T_1^{20}	T_{dep}^N	T_{dep}^{42}	T_{dep}^{20}	T_{dep}^V
(a) 16.16	(a) 16.40	(a) 16.20	(CII) 15.83	6.1[b]	6.0	5.6	A	A	A	A
(b) 16.16	(b) 15.77	(b) 16.15	(CI) 16.50	2.7[b]	2.8	2.8	A	A	A	A
(c) 12.61	(c) 12.80	(c) 12.64	(CIII) 12.66	7.5	7.3	7.5	A	A	A	A
(d) 10.80	(d) 10.80	(d) 10.97		2.2	2.1	2.3	A	A	A	A
(e) 10.05	(e) 10.10	(e) 9.93		2.2	2.1	2.2	A	A	A	A
(f) −0.32	(f) −0.33	(f) −0.33		7.4	7.9	7.9	C	C	C	
	(g) 15.99	(g) 12.43			26.0	33.0		C	C	
	(h) −1.74				10.6			C		
	(i) −34.17	(h) −35.96			1.5	1.5		C	C	

[a] pH 7.2; T_1 values are in milliseconds. N = native HiPIP from *C. gracile*; 42 = Ru(His-42); 20 = Ru(His-20); V = native HiPIP from *C. vinosum*; C = Curie behavior; A = anti Curie behavior; T_{dep} = temperature dependence. [b] Determined at pH 9.

determining the different redox properties of these two classes of proteins (Nettesheim et al., 1983). The most extensively characterized example of a high-potential protein is that from the photosynthetic bacterium *Chromatium vinosum* (Carter et al., 1974; Dus et al., 1967, 1973; Mizrahi et al., 1976). The high-resolution X-ray crystal structures by Carter and coworkers (Carter et al., 1974) have provided many valuable insights on the possible role of structural factors in the modulation of the cluster potential. Other physical techniques have been used to probe for conserved properties of this class of protein that may be involved in the determination of redox properties. NMR has been extensively used in this respect, and the ^{1}H NMR spectra of HiPIP's from *C. vinosum*, *Rhodopseudomonas gelatinosa* (Nettesheim et al., 1983), *Ectothiorhodospira halophila*, and *Ectothiorhodospira vacuolata* (Krishnamoorthi et al., 1986) have been reported. Several attempts have been made to rationalize the behavior of the isotropically shifted signals. The influence of histidine ionization (Nettesheim et al., 1983) and the stabilization of the cluster by hydrogen bonds and $\pi-\pi$ interactions (Krishnamoorthi et al., 1986) have all been monitored, although a reliable interpretation of the subtle spectral differences between HiPIP's and Fd's, in terms of the different structural properties modulating the reduction potential, has been lacking.

The HiPIP from *C. gracile* contains a 74% amino acid sequence homology with that from *C. vinosum* (Dus et al., 1967) and has not been previously studied by NMR. In this paper we describe a detailed characterization of the *C. gracile* protein by ^{1}H NMR, including the effects of varying pH and temperature, the measurement of relaxation times, and the correlation of resonances in the oxidized and reduced forms by saturation-transfer experiments. From this comprehensive study, we outline either conclusive or tentative assignments of all the isotropically shifted signals to specific residues, in both the reduced and oxidized forms, and reassign some previously reported signals in homologous HiPIP's. Furthermore, we present evidence for an additive pH influence of several ionizable residues around the cluster, map out the distribution of delocalized spin density on the cluster and its immediate environment, and use this to propose a model that accounts for the pH modulation, and differing values, of the reduction potentials of both HiPIP's and Fd's. We also have investigated ruthenium-modified derivatives of *C. gracile* HiPIP (J. A. Cowan, S. Harder, R. G. Bartsch, B. A. Feinberg, and H. B. Gray, unpublished results); the NMR spectra of these ruthenated proteins have proved useful in the interpretation of pH effects of individual ionizable residues.

Experimental Procedures

Protein Isolation. *C. gracile* (strain HOL1, P. F. Weaver) was grown as described by Bartsch (1971, 1978) and the protein extracted from the cell paste by a modification of the procedure reported by Bartsch for *C. vinosum* HiPIP (Bartsch, 1978; Cowan et al., unpublished results). The preparation of ruthenium-modified derivatives shall be discussed elsewhere (Cowan et al., unpublished results).

NMR Measurements. Spectra were recorded on a Bruker AM 500 instrument operating at 500.13 MHz. Protein samples (2–4 mM) were generally run in 99% D_2O, containing sodium phosphate as buffer (μ = 100 mM). A solvent mixture of 90% H_2O and 10% D_2O (by volume) was used to identify the exchangeable protons. Typically, 1000–3000 transients were accumulated by using a 90° pulse (6.3 μs) with a delay time of 0.5 s between pulses. Solvent suppression was achieved by a presaturation pulse from the decoupler. In saturation-transfer experiments, efficient D_2O exchange obviated the need for solvent suppression. Chemical shifts were internally referenced to 2,2-dimethyl-2-silapentane-5-sulfonate (DSS). The pH of samples was varied by the addition of small amounts of NaOD or DCl. pH values were measured both before and after the transient accumulation with a Metrohm 6.0204.100 combined glass electrode and were not corrected for the deuterium isotope effect. The pK_a values for the two titration steps present in the oxidized forms were obtained separately by fitting the appropriate data sets to an equation for a single ionization equilibrium $[\delta(\text{pH}) = \delta_{HA}[H^+]/(K_a + [H^+]) + \delta_A K_a/(K_a + [H^+])]$, using a nonlinear least-squares program. T_1 relaxation times were determined by using the usual inversion-recovery method, with τ values in the range 0.1–200 ms, and fitting the intensity values to the equation $M_z = M_0[1-2\exp(-\tau/T_1)]$. Saturation-transfer experiments were performed on mixtures containing both oxidized and reduced species (ratio 1:1) that were obtained by adding increasing amounts of $K_3Fe(CN)_6$ to the initially fully reduced samples and checking the ratio of oxidized:reduced protein from the area of corresponding signals.

Results

Native. The hyperfine-shifted signals of the reduced protein at pH 5.6 are shown in Figure 1. The five resonances (a–e) observed in the downfield region all display anti Curie behavior (Figure 2, T_{dep}^N Table I). Resonances a–d are found at chemical shifts similar to those found for *C. vinosum* HiPIP (Nettesheim et al., 1983) (Table I), although resonance e, which lies under two slowly exchangeable protons, can only be detected after several hours of D_2O exchange and had not been previously observed. The sharp resonance at 10.7 ppm does not show a temperature dependence and remains at the same chemical shift in the oxidized protein; therefore, it is unaffected by the paramagnetic cluster. There is an additional hyperfine-shifted resonance (f) in the upfield region that displays Curie behavior and integrates to two protons (the diamagnetic background also makes a minor contribution). The high-field signal (−0.7 ppm), having no temperature de-

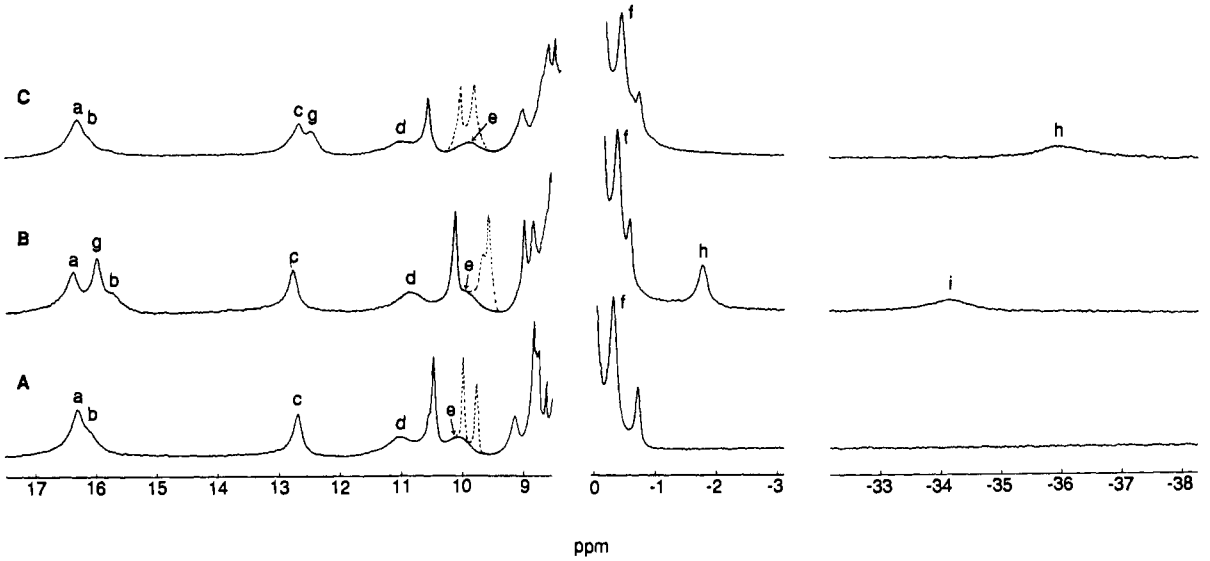

FIGURE 1: 500-MHz ^1H NMR spectra of reduced HiPIP from *C. gracile* in D_2O: (A) native protein, pH 5.6; (B) Ru^{III}(His-42) derivative, pH 7.2; (C) Ru^{III}(His-20) derivative, pH 7.2. The diamagnetic region is not shown. T = 25 °C. Signals due to exchangeable protons are dotted. The spectrum of the native protein is reported at pH 5.6. At neutral pH signals a and b are completely overlapped and signal d is less well resolved from the diamagnetic region.

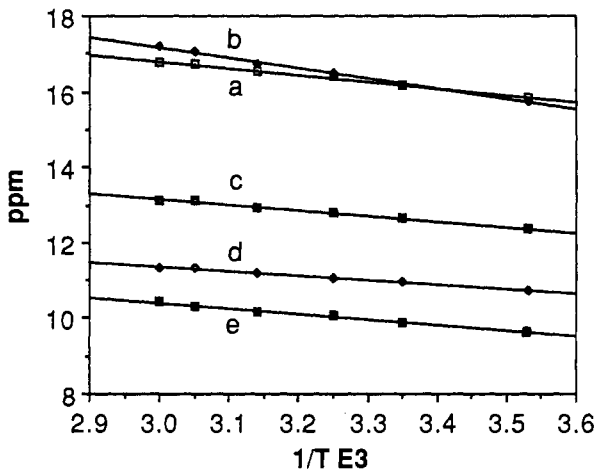

FIGURE 2: Curie plots for the hyperfine-shifted signals of reduced native HiPIP, pH 7.2.

pendence and a T_1 value of 290 ms, is not isotropically shifted.

The curves illustrating the pH dependence of the hyperfine-shifted resonances (Figure 3) show a small titration step with an apparent pK_a of 7.6. The pH dependence of signals d and e is not shown since the signals were too broad for accurate determination of chemical shift. Signal f shows no pH dependence. This pattern has also been obtained for the HiPIP from *C. vinosum* and had been assigned to the deprotonation of the pyridine nitrogen of His-42 (pK_a = 7.3) (Nettesheim et al., 1983). In the protein from *C. gracile*, a second solvent-exposed histidine (His-20) is present that also lies close to the cluster; thus, the involvement of both histidines in the titration step cannot be excluded. This particular point will be clarified by analysis of the results from the pH dependence of the corresponding resonances in each of the ruthenium derivatives.

The influence of the glutamic acid residue (Glu-44) is also evident from the pH study. A careful titration in the range pH 5–7 revealed an inflection in the pH behavior of the sharpest peaks (a and c) with an apparent pK_a of 5.8 that can be assigned to the ionization of this residue. No such effect was observed in studies of the *C. vinosum* protein, since in this case an alanine residue is found at position 44 (Carter et al., 1974). In addition, Glu-44 is closer to the cluster than other surface acidic residues; its presence might also explain the higher pK_a obtained for His deprotonation in the *C. gracile* protein relative to that for *C. vinosum*.

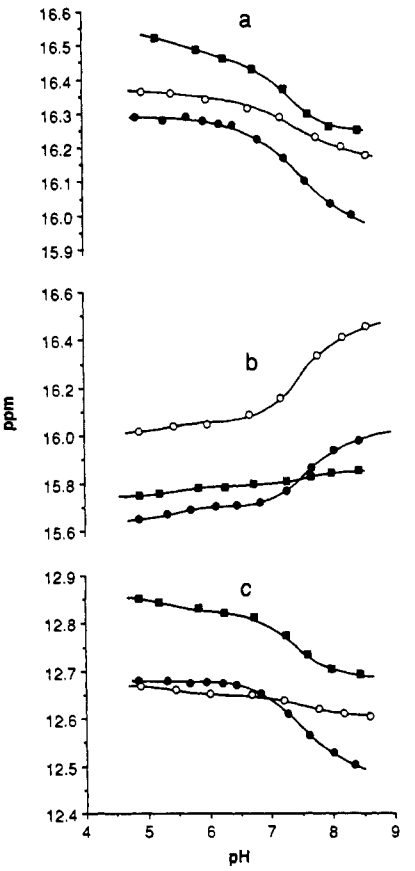

FIGURE 3: pH dependences of the hyperfine-shifted resonances of reduced HiPIP: (●) native protein; (■) Ru^{III}(His-42) derivative; (○) Ru^{III}(His-20) derivative.

Further evidence for the influence of histidine deprotonation on the $[Fe_4S_4]$ cluster is derived from the temperature dependence of the isotropically shifted signals determined at different pH's (Figure 4). When the paramagnetic shift is contact in origin, the gradient of the Curie plot is directly

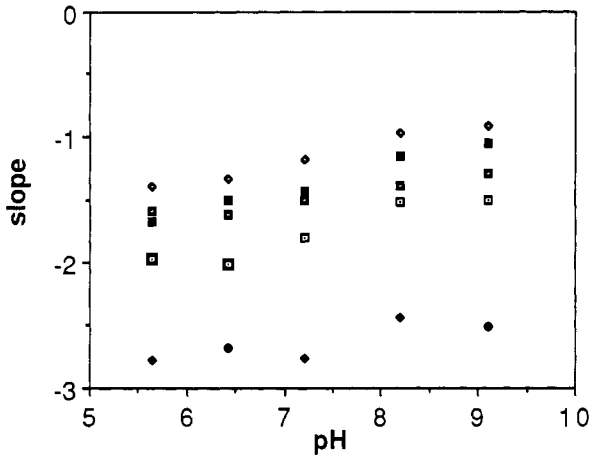

FIGURE 4: pH dependences of the slopes in the Curie plots of the hyperfine-shifted signals in native HiPIP: (⊡) ppm a; (◆) ppm b; (◘) ppm c; (◈) ppm d; (■) ppm e.

related to the Fermi coupling constant (Jesson, 1973), and this is also valid for antiferromagnetically coupled systems (La Mar et al., 1973). For each of the hyperfine-shifted resonances in the *C. gracile* protein, the slopes obtained at different pH's show a clear titration pattern with an apparent pK_a of 7.5, in excellent agreement with that observed in the "direct" pH titration. This clearly indicates that the pH dependence of the chemical shift of the hyperfine-shifted signals reflects changes in the electronic properties of the cluster, although the possibility of simultaneous conformational changes cannot be excluded.

The spectrum of the oxidized protein is shown in Figure 5, and the NMR parameters are reported in Table II. The downfield region shows a pattern of five resonances in the 20–40 ppm region and a very low shifted signal at ca. 100 ppm, integrating to a total of seven protons. Four signals are observed in the high-field region; however, two of these (at −8.0 and −19.2 ppm) slowly disappear with time (20 h) and can be assigned to exchangeable protons. The temperature dependence of the hyperfine-shifted signals (Figure 6) exhibits Curie behavior for all signals other than g and h, which show anti Curie behavior. The overall appearance of the spectrum is similar to that for other HiPIP's, and in particular with those from *E. vacuolata* (Krishnamoorthi et al., 1986) and *C. vinosum* (Nettesheim et al., 1983).

The HiPIP from *C. gracile* has a 74% amino acid sequence homology with that from *C. vinosum*, and the conserved resonances can be readily assigned. In particular, from the work of Nettesheim et al. (1983) signals a, e, and f clearly correspond to C1, C8, and C9, respectively, signal b (two protons) corresponds to the doublet C2 and C3, signals c and d correspond to C4 and C5, while signals g and h, the only signals showing anti Curie behavior, must correspond to C6 and C7. In general, with the exception of signals g and h, correlated resonances from the *C. gracile* protein exhibit smaller isotropic shifts than those in *C. vinosum* HiPIP. The differences in the primary structure of these two proteins are therefore sufficient to induce some changes in the pattern of the isotropically shifted signals, but are not large enough to result in a substantial conformational change. This conclusion is supported by molecular graphics analysis of the *C. vinosum* and energy-minimized *C. gracile* structures. Use of the BIOGRAF software package (Biodesign, Inc.) allowed the two residues in the *C. vinosum* sequence that are absent from *C. gracile* to be deleted, and the terminal atoms were joined by a bond.

As a result of the larger paramagnetism of the oxidized protein, the signals show an increased pH dependence in comparison with the reduced form, and the two titration steps

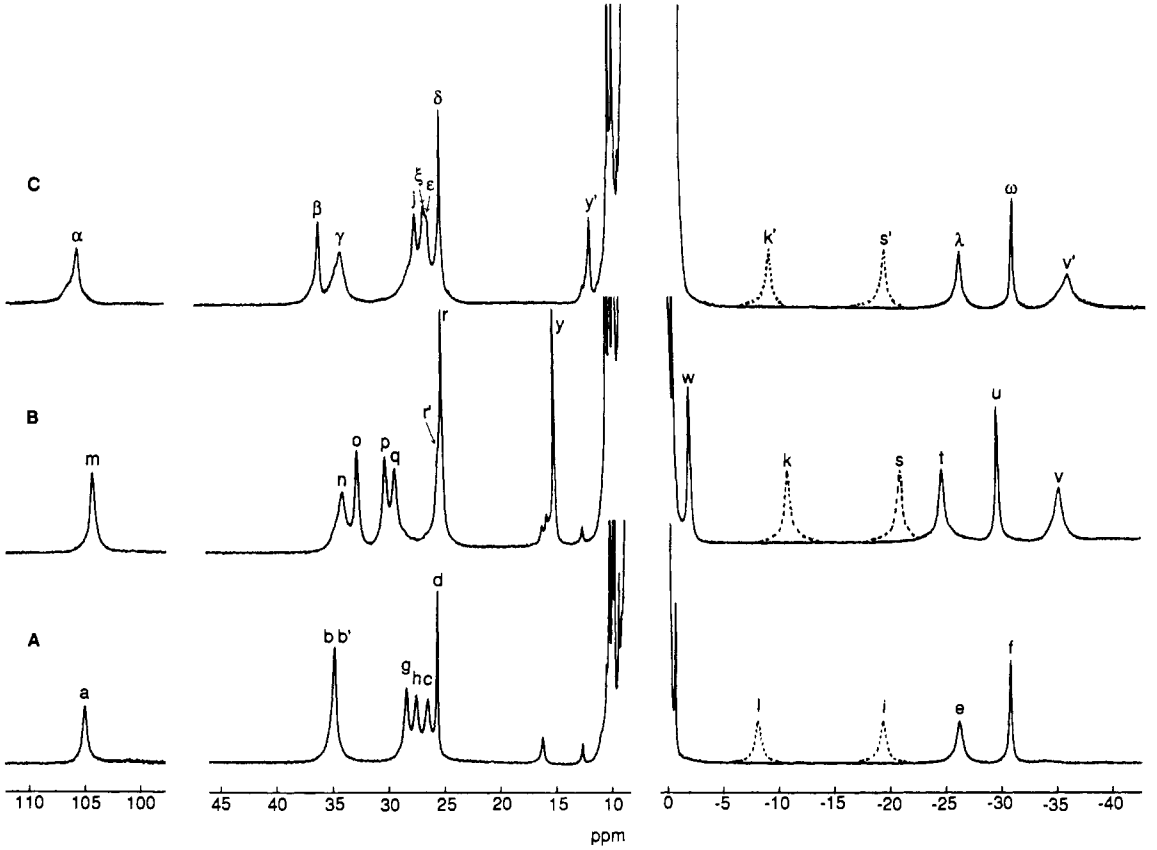

FIGURE 5: 500-MHz ^1H NMR spectra of oxidized HiPIP from *C. gracile* in D_2O, pH 7.2, T = 25 °C: (A) native protein; (B) Ru^{III}(His-42) derivative; (C) Ru^{III}(His-20) derivative. The diamagnetic region is not shown. Exchangeable protons are dotted.

Table II: ^{1}H NMR Parameters of the Oxidized Form of Native HiPIP from *C. gracile* and Its Ru(III) Derivatives[a]

ppm^N	ppm^{42}	ppm^{20}	ppm^V	T_1N	T_1^{42}	T_1^{20}	T_{dep}^N	T_{dep}^{42}	T_{dep}^{20}	T_{dep}^V
(a) 105.03	(m) 104.32	(a) 105.77	(C1) 107.3	7.0	6.8	6.8	C	C	C	C
(b) 36.65[b]	(n) 34.28	(γ) 34.45	(C3) 36.79	6.2[b]	5.3	4.5	C	C	C	C
(b′) 35.61[b]	(o) 32.94	(β) 36.42	(C2) 39.20	16.0[b]	19.0	17.4	C	C	C	C
(c) 26.50	(r′) 25.50	(ϵ) 26.66	(C4) 30.06	8.6	21.0	8.6	C	C	C	C
(d) 25.65	(r) 25.27	(δ) 25.49	(C5) 27.43	40.7	49.8	46.3	C	C	C	C
(g) 28.40	(p) 30.41	(j) 27.74	(C6) 25.38	8.9	9.4	9.6	A	A	A	A
(h) 27.53	(q) 29.55	(ζ) 26.94	(C7) 24.61	8.4	8.6	8.4	A	A	A	A
(l) −8.00[c]	(k) −10.43[c]	(k′) −9.30[c]								
(i) −19.24[c]	(s) −20.75[c]	(s′) 19.12[c]								
(e) −26.27	(t) −24.51	(λ) −26.06	(C8) −32.70	14.1	13.7	14.2	C	C	C	C
(f) −30.86	(u) −29.53	(ω) −30.81	(C9) −33.30	40.1	38.0	41.0	C	C	C	C
	(v) −35.09	(v′) −35.85			1.5	1.5		C	C	
	(y) 15.25	(y′) 12.01			23.0	29.0		C	C	
	(w) −2.1							C		

[a] pH 7.2; T_1 values are in milliseconds. N = native HiPIP from *C. gracile*; 42 = Ru(His-42) derivative; 20 = Ru(His-20) derivative; V = native HiPIP from *C. vinosum*; C = Curie behavior; A = anti Curie behavior; T_{dep} = temperature dependence. [b] Values at pH 9. At pH 7.2 the overlapping peaks lie at 34.83 ppm with a T_1 of 10.9 ms. [c] Exchangeable protons.

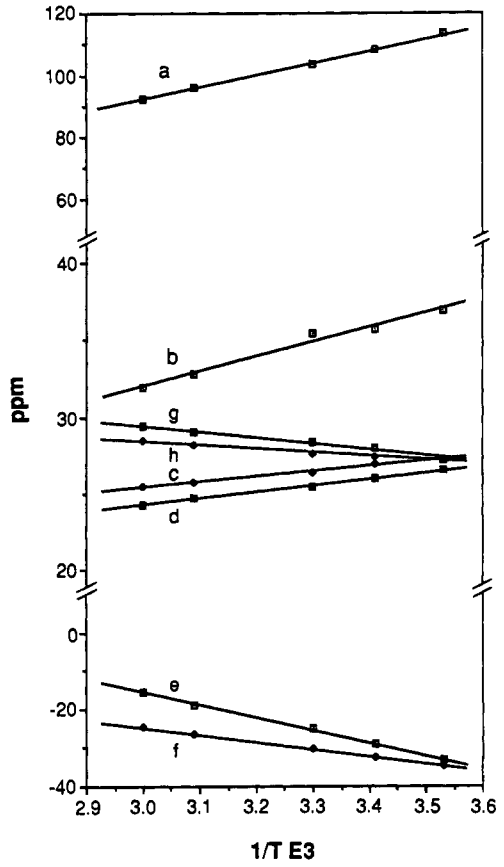

FIGURE 6: Curie plots for the hyperfine-shifted signals of oxidized native HiPIP, pH 7.2. Similar patterns were obtained for both of the Ru^{III}(His) derivatives.

with pK_a's of 5.8 and 7.0 are now clearly observable (Figure 7). While the first may be confidently attributed to the ionization of Glu-44, the second is characteristic of histidine deprotonation; its pK_a is larger than that determined for the *C. vinosum* protein (pK_a = 6.7) (Nettesheim et al., 1983), most probably because of the presence of the negatively charged Glu-44.

Ru^{III}(His-42)HiPIP (*C. gracile*). The spectrum of the reduced protein (Figure 1B) displays three new signals at δ 15.99 (g), −1.74 (h), and −34.17 (i). In comparison to the native protein, the remaining signals show little change in position. In particular, signals a, c, and d experience a downfield shift, while signal b is shifted upfield; line widths, T_1 values, and variable-temperature behavior, are the same (Table I). The nature of the pH dependence is qualitatively similar to that of the native protein (Figure 3), although the chemical shift variations between pH 5 and 9 are smaller. The titration step at pH ~7 is still present and clearly indicates that the second histidine residue (His-20) influences the cluster. The pK_a values are practically unchanged as compared to the native protein with pK_a's of 5.8 and 7.4 and indicate that the positive charge on the ruthenium ion does not have an appreciable electrostatic influence on the His-20 residue. The possible influence of Ru(III) on the ionization of Glu-44 may be obscured by the very weak chemical shift response to changes in pH.

In comparison with native protein, the general features of the spectrum of the oxidized derivative are unchanged. The three new signals observed in the reduced form (g, h, and i) are still present in the oxidized form (y, w, and v), with approximately the same chemical shift. For those signals where assignments of the corresponding resonances in the native protein can be safely made [m(a), t(e), u(f) (Table II)], the ruthenium-induced shifts are slightly greater than those observed in the reduced form, although they are not in the same direction. As for the reduced protein, the ruthenium(III) affects neither the variable-temperature behavior (only slightly greater slopes are detected in the Curie plots) nor the relaxation properties of the resonances. The assignment of corresponding signals in the ruthenium derivative and the native protein can also be readily carried out in the 20–40 ppm region. In particular, signals b and b′ correspond to n and o, resonances g and h (showing anti Curie behavior) correspond to the analogous p and q, signal d corresponds to r, and signal c corresponds to r′. In general, no variations were observed in the relaxation characteristics of signals other than c (in which case the T_1 of the corresponding resonance r′ may be influenced by the closely overlapping signal r, which has a long relaxation time).

The pH titration of the isotropically shifted resonances still shows two steps, with pK_a's of 5.8 and 6.9, attributable to the ionization of Glu-44 and His-20, respectively. As was the case for the reduced form, both pK_a's are unaffected by the presence of the ruthenium ion.

Ru^{III}(His-20)HiPIP (*C. gracile*). The spectra of the reduced and oxidized protein are shown in Figures 1C and 5C, respectively. The general observations made for the spectral features of the His-42-labeled protein can also be made for this derivative, although the chemical shift variations, in comparison to those in the native protein, are smaller. In this case, only two new signals were observed, rather than three, and the shifts were again independent of oxidation state. The hyperfine-shifted resonances titrate with pK_a values of 5.8 and

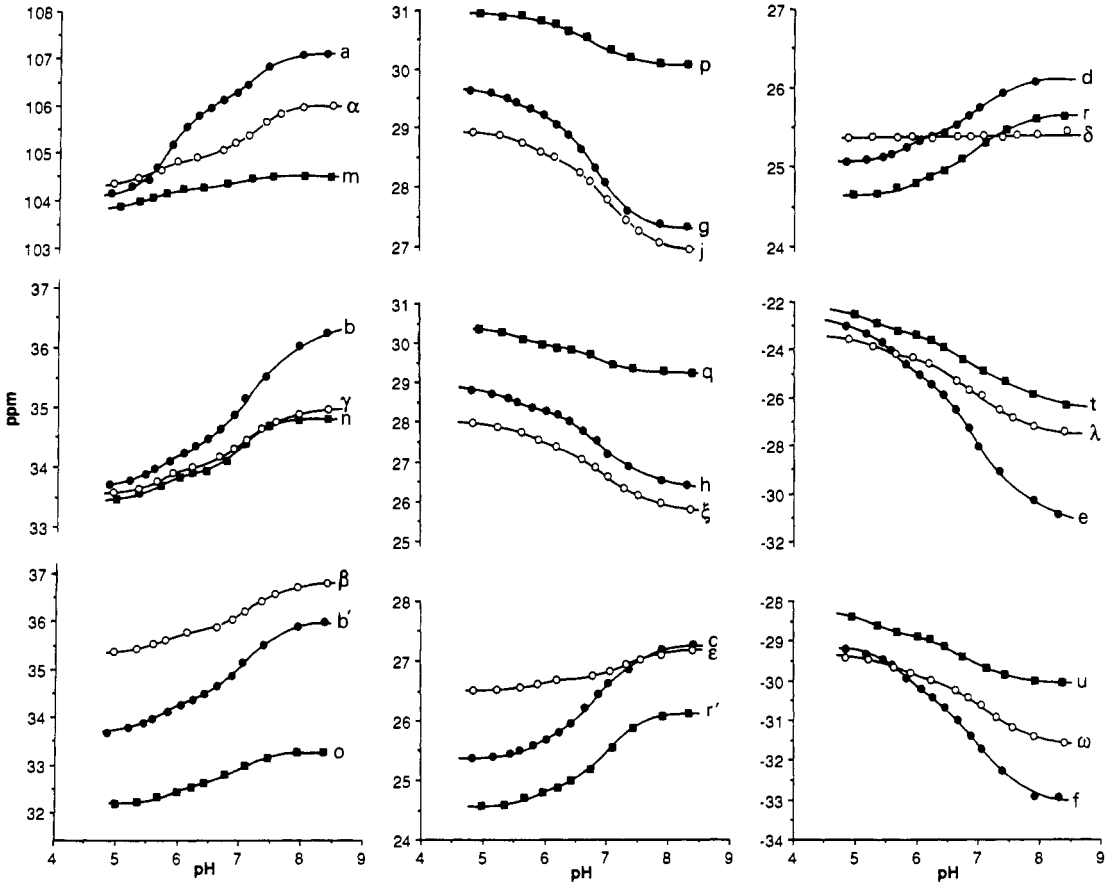

FIGURE 7: pH dependences of the hyperfine-shifted resonances of oxidized HiPIP: (●) native protein; (■) Ru^{III}(His-42) derivative; (○) Ru^{III}(His-20) derivative.

7.5 in the reduced form and 5.8 and 7.1 in the oxidized form.

Discussion

Reduced Native. In frozen solution at 200 K, the reduced form of native HiPIP is diamagnetic due to antiferromagnetic coupling between the iron atoms of the cluster by an exchange or superexchange mechanism, the latter involving the sulfide bridges (Moss et al., 1969). At ambient temperature, the increased population of magnetic states results in the observation of isotropically shifted resonances. Accordingly, the downfield set of signals shows anti Curie behavior (Figure 2) that parallels the increase in the magnetic susceptibility (Holm et al., 1974). The T^{-1} dependence, the very low magnetic anisotropy of the $[Fe_4S_4]$ cluster, and comparison with the results from extensive investigations on synthetic analogues (Holm et al., 1974; Que et al., 1974; Reynolds et al., 1978; Laskowski et al., 1978) indicate that the electron–nucleus coupling is predominantly contact in origin.

Four downfield resonances have normally been detected in previous studies of HiPIP's (Nettesheim et al., 1983; Phillips et al., 1970) and invariably have been assigned to the β-CH_2 protons of the four cysteine residues directly coordinated to the cluster. The observation of less than eight protons is consistent with the angular dependence of the contact coupling constant. The fixed orientation of the CH_2 groups restricts each proton to different regions of orbital overlap and leads to widely different chemical shift values for the isotropically shifted resonances (Poe et al., 1970). We have now detected a fifth signal (e) that can be assigned to either another β-CH_2 proton or one from a different residue very close to the cluster. The upfield signal f may be assigned to protons experiencing π–π interactions with the cluster, most probably from a nearby aromatic residue.

Oxidized Native. The increased paramagnetism of the oxidized form (magnetic susceptibility corresponding to one unpaired electron at 200 K) (Moss et al., 1969) results in the appearance of a large number of isotropically shifted resonances, both downfield and upfield of the diamagnetic region. The presence of upfield signals indicates that a π spin-transfer mechanism contributes to the contact shift (Bertini et al., 1986). We assign the signals a, b, g, and h, which have low T_1 values and are the most downfield-shifted resonances, to four β-CH_2 protons. Each of these protons probably belongs to a different cysteine residue, due to the previously cited angular overlap dependence of the hyperfine coupling constant.

The anti Curie behavior of signals g and h is of particular interest. The heterogeneous temperature behavior of the hyperfine-shifted signals in oxidized HiPIP's has been previously explained by assuming the unpaired spin to be incompletely delocalized over the cluster and to reside primarily around two iron centers, two sulfide bridges, and two cysteine residues (Phillips et al., 1970). An alternative is to assign the anti Curie signals to aromatic protons that experience π–π interaction with the cluster (Krishnamoorthi et al., 1986). We propose, in line with the former interpretation, that protons g and h belong to two cysteine β-CH_2 groups that are influenced by the antiferromagnetic coupling of the other two iron centers in the cluster. This assignment is consistent with the higher T_1 values of these signals in comparison with those for the other two β-CH_2 groups and is supported by saturation-transfer experiments performed on the half-reduced/half-oxidized protein (Figure 8). The electron-exchange rate is relatively high ($k_{ex} \sim 1.7(4) \times 10^4$ M^{-1} s^{-1}), but it allows detectable changes in the intensities of corresponding signals. Signals g, h, a, and b correspond to four of the five isotropically shifted downfield resonances of the reduced form, and all can

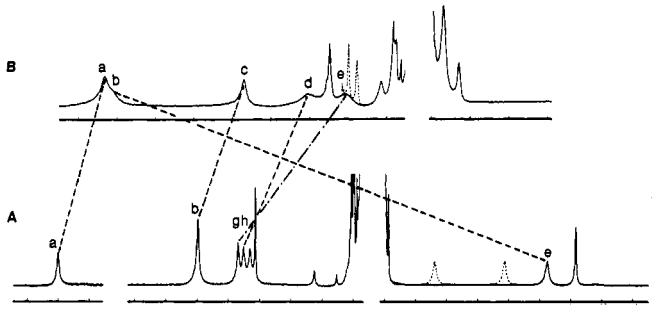

FIGURE 8: Results of saturation-transfer experiments on native HiPIP from *C. gracile*, pH 5.2: (A) oxidized form; (B) reduced form.

therefore be confidently assigned to four β-CH_2 protons. The lack of a uniform distribution of spin density could be regarded as the origin of the relative instability of the oxidized state in comparison to the reduced one, which is reflected in the high positive reduction potential of this class of proteins. Similar arguments apply to Fd's relative to their reduced state (Phillips et al., 1974; Moura et al., 1977; Poe et al., 1971): these display the same mixed-temperature behavior of the isotropically shifted signals, so the instability of this state may be considered responsible for the high negative reduction potential of Fd's. Thus, while the presence of different redox couples in HiPIP's and Fd's is undoubtedly due to *different* hydrophobic and hydrogen-bond interactions between the polypeptide chain and the cluster (Palmer, 1975; Carter et al., 1972; Sheridan et al., 1981), the stability of the reduced and oxidized states, respectively, which correspond to the same cluster oxidation level, must arise from a *common* feature in the cluster–polypeptide backbone interaction[1] that does not allow a complete delocalization of the unpaired spin over the cluster when an electron is added (Fd's) or removed (HiPIP's) from the common "paired-spin state" $[Fe_4S_4(SCys)_4]^{2-}$.

The above assignment of the signals g and h would also readily account for the correspondence between their anti Curie behavior and their opposite pH dependence, in comparison with the other resonances [also observed for the HiPIP from *C. vinosum* (Nettesheim et al., 1983)]. The decrease in the hyperfine shift of these protons with increasing pH (Figure 7) could be due to a further movement of the unpaired spin density to the opposite side of the cluster (relative to these protons), due to the electronic effects exerted by the deprotonation of the Glu-44 and the His residues. This would result in an increased isotropic shift of the other Cys protons. In addition, the possibility of partial spin delocalization over the Tyr-19 residue, which is known to be in van der Waals contact with the cluster, could lead to a stabilization of the oxidized form with increasing pH and account for the observed decrease in the reduction potential for the homologous HiPIP from *C. vinosum* (Mizrahi et al., 1976). The pH dependences of the reduction potential (Mizrahi et al., 1976) and chemical shifts (Nettesheim et al., 1986) in *C. vinosum* are in reasonable agreement except at low pH ($\sim$5), where other factors, including protein stability and the divergence of electrostatic and magnetic interactions, may contribute. We assign signal e in the oxidized form of the protein to a proton of Tyr-19; its upfield position, short relaxation time (13 ms), and "abnormal" intercept in the Curie plot (96 ppm) are indicative of a proton that is experiencing a strong π–π interaction with the cluster (Krishnamoorthi et al., 1986). Saturation-transfer experiments show that this signal corresponds to signal b in the reduced form, which consequently cannot be a β-CH_2 proton as previously assigned. Signal b can also be distinguished from the other four downfield signals by the opposite trend of its pH dependence (Figure 3). The appearance of Tyr-19 in the spectrum of the reduced form (which shows a residual paramagnetism) is consistent with the very short distance of this residue from the cluster. In the oxidized form, the pH dependence of the chemical shift of signal e is almost 4 times greater than the average value shown by the other signals and supports the above arguments on the delocalization of spin density over Tyr-19 with increasing pH.

In the oxidized form, signal a corresponds to the β-CH_2 proton that displays the largest chemical shift dependence on the ionization of Glu-44. We therefore can assign this resonance, and the corresponding one in the reduced protein, to a Cys-43 β-CH_2 proton. Since this Cys-43 resonance exhibits Curie behavior, it must correspond to one of the residues coordinated to the portion of the cluster that is influenced by the localization of the unpaired spin density. From the X-ray structure of *C. vinosum* (Carter et al., 1974a,b), Cys-43 and Cys-77 are the iron-bound residues that face the aromatic ring of Tyr-19. This finding supports the above idea of spin-density delocalization from the "electron-rich" side of the cluster to Tyr-19 with increasing pH. The other β-CH_2 signal (b) displaying Curie behavior can therefore be assigned to Cys-77. Consequently, signals g and h should correspond to the β-CH_2 groups of the other two Cys residues, 46 and 63. Evans and co-workers (Evans et al., 1970) have previously detected a quadrupole-split doublet in Mössbauer experiments on the *C. vinosum* protein and have proposed a slight inequivalence between the two sets of iron centers. This pairwise inequivalence was found for both of the available redox states of the cluster, and a uniform change in electron density at each iron center was noted on oxidation or reduction. The observation of two discrete types of iron centers is in accord with our analysis of the delocalization of unpaired electron spin over the cluster.

Both signals b′ and c show significant isotropic shifts and have short T_1 values (most noticeably for signal c). Each of these resonances could, therefore, correspond to Tyr-19 protons that have moved toward the cluster following oxidation of the protein. Alternatively, signal c could be assigned to a second proton from a β-CH_2 cysteine group (43 or 77). Due to its long T_1, signal d can be assigned to a proton from the polypeptide backbone surrounding the cluster. The resonances at −8.0 and −19.24 ppm, which slowly disappear with time in D_2O, have already been observed in other HiPIP's (Krishnamoorthi et al., 1986) and can generally be assigned to hyperfine-shifted protons that are hydrogen bonded to the cysteine sulfur atoms (Carter et al., 1974a).

Signal f has a long T_1 and a normal diamagnetic intercept in the Curie plot and lies in the upfield region. We therefore agree with the previous assignment to an α-CH proton (Krishnamoorthi et al., 1986): i.e., the relatively large hyperfine shift is consistent with a π spin delocalization mechanism in which the sign of the spin density alternates between positions and the magnitude of the isotropic shift does not necessarily attenuate as the distance from the paramagnetic center is increased.

Ruthenium Derivatives. In the ruthenium derivatives, the broad upfield signal at ca. −35 ppm may be assigned to the C-2 proton of the histidine residue bearing the Ru(III) ion; the same signal has been observed and assigned in both Ru(III)-labeled sperm whale myoglobin (Mb) and a model compound $[a_5Ru(III)Im]$ (Toi et al., 1984). The new signals

[1] In the synthetic analogues $[Fe_4S_4(SR)_4]^{3-}$, only Curie behavior is detected [Reynolds et al., (1978)].

observed in the ruthenium derivatives (e.g., g, h, i and y, w, v for the reduced and oxidized His-42 derivative, respectively) have the same chemical shift and relaxation properties in both the oxidized and reduced states of the protein cluster and can be assigned to Ru(III)-shifted protons, presumably belonging to aromatic residues surrounding the ion.

Other than the appearance of new resonances, the introduction of the Ru(III) center gives rise to only slight chemical shift changes [that are very small indeed for the Ru(His-20) derivative] and does not influence the relaxation properties of the signals. It is therefore reasonable to assume that the spectra of the ruthenium-labeled derivatives can be assigned by reference to those described above for the native protein. Furthermore, this comparison points out the absence of any significant magnetic interaction between the cluster and the surface ruthenium ion. The slightly different chemical shift values can thus be attributed to minor conformational changes. The absence of significant perturbations in the NMR spectrum of a protein following ruthenium modification has been noted previously for myoglobin (Toi et al., 1984). In that case, no chemical shift changes were observed, although slight enhancements of the relaxation rates were attributed to a minor interaction between the two metal centers.

In both of the ruthenium derivatives the chemical shift variation between pH 5.0 and 8.5 is lower than that of the native protein, indicating that the deprotonation of both histidines influences the cluster. Within experimental error, and for both oxidation states, the ruthenium derivatives also show a pH dependence that is complementary to that of the native protein (due to protonation of the free His) and confirms that the introduction of the ruthenium ion does not give rise to significant changes in protein conformation. This comparison also indicates that particular signals can experience quite different influences from the two histidines.

Conclusions. We have assigned the isotropically shifted resonances in the ^{1}H NMR spectra of both oxidized and reduced states of the HiPIP from *C. gracile*. These signals correspond to specific β-CH_2 protons of the cysteine residues binding the $[Fe_4S_4]$ cluster and to surrounding aromatic residues (Tyr-19 in particular). Three ionizable sites (His-42, His-20, and Glu-44) play an active role in modulating the electronic properties of the cluster, and evidence has been presented for the involvement of Tyr-19 as an acceptor of spin density. We believe that the nonuniform spin distribution over the cluster is an important factor in the determination of the redox properties of HiPIP's and Fd's. The spectra of the ruthenated derivatives indicate that coordination of ruthenium to a surface histidine does not significantly alter the protein conformation.

Registry No. L-His, 71-00-1; L-Glu, 56-86-0.

References

Bartsch, R. G. (1971) *Methods Enzymol. 23*, 644–649.

Bartsch, R. G. (1978) *Methods Enzymol. 53*, 329–340.

Bertini, I., & Luchinat, C. (1986) in *NMR of Paramagnetic Molecules in Biological Systems* (Lever, A. B. P., & Gray, H. B., Eds.) Vol. 3, pp 18–44, Benjamin/Cummings, Menlo Park, CA, and references therein.

Carter, C. W., Jr. (1977) in *Iron-Sulfur Proteins* (Lovenberg, W., Ed.) Vol. 3, pp 157–204, Academic Press, New York.

Carter, C. W., Jr., Kraut, J., Freer, S. T., Alden, R. A., Sieker, L. C., Adman, E., & Jensen, L. H. (1972) *Proc. Natl. Acad. Sci. U.S.A. 69*, 3526–3529.

Carter, C. W., Jr., Kraut, J., Freer, S. T., Xuong, N.-H., Alden, R. A., & Bartsch, R. G. (1974a) *J. Biol. Chem. 249*, 4212–4225.

Carter, C. W., Jr., Kraut, J., Freer, S. T., & Alden, R. A. (1974b) *J. Biol. Chem. 249*, 6339–6346.

Dus, K., DeKlerk, H., Sletten, K., & Bartsch, R. G. (1967) *Biochim. Biophys. Acta 140*, 291–311.

Dus, K., Tedro, S., & Bartsch, R. G. (1973) *J. Biol. Chem. 248*, 7318–7331.

Evans, M. C. W., Hall, D. O., & Johnson, C. E. (1970) *Biochem. J. 119*, 289–291.

Holm, R. H., Phillips, W. D., Averill, B. A., Mayerle, J. J., & Herskovitz, T. (1974) *J. Am. Chem. Soc. 96*, 2109–2117.

Jesson, J. P. (1973) in *NMR of Paramagnetic Molecules* (La Mar, G. N., Horrocks, W. D., Jr., & Holm, R. H., Eds.) pp 2–51, Academic Press, New York.

Krishnamoorthi, R., Markley, J. L., Cusanovich, M. A., Przysiecki, C. T., & Meyer, T. E. (1986) *Biochemistry 25*, 60–67, and references therein.

La Mar, G. N., Eaton, G. R., Holm, R. H., & Walker, F. A. (1973) *J. Am. Chem. Soc. 95*, 63–75.

Laskowski, E. J., Frankel, R. B., Gillum, W. D., Papaefthymiou, G. L., Renaud, J., Ibers, J. A., & Holm, R. H. (1978) *J. Am. Chem. Soc. 100*, 5322–5337.

Meyer, T. E., Przysiecki, C. T., Watkins, J. A., Bhattacharyya, A., Simondsen, R. P., Cusanovich, M. A., & Tollin, G. (1983) *Proc. Natl. Acad. Sci. U.S.A. 80*, 6740–6744.

Mizrahi, I. A., Wood, F. E., & Cusanovich, M. A. (1976) *Biochemistry 15*, 343–348.

Moss, T. H., Petering, D., & Palmer, G. (1969) *J. Biol. Chem. 244*, 2275–2277.

Moura, J. J. G., Xavier, A. V., Bruschi, M., & Le Gall, J. (1977) *Biochim. Biophys. Acta 459*, 278–289.

Nettesheim, D. G., Meyer, T. E., Feinberg, B. A., & Otvos, J. D. (1983) *J. Biol. Chem. 258*, 8235–8239, and references therein.

Palmer, G. (1975) *Enzymes (3rd Ed.) 12B*, 1–56.

Phillips, W. D., Poe, M., McDonald, C. C., & Bartsch, R. G. (1970) *Proc. Natl. Acad. Sci. U.S.A. 67*, 682–687.

Phillips, W. D., McDonald, C. C., Stombaugh, N. A., & Orme-Johnson, W. H. (1974) *Proc. Natl. Acad. Sci. U.S.A. 71*, 140–143.

Poe, M., Phillips, W. D., McDonald, C. C., & Lovenberg, W. (1970) *Proc. Natl. Acad. Sci. U.S.A. 65*, 797–804.

Poe, M., Phillips, W. D., McDonald, C. C., & Orme-Johnson, W. H. (1971) *Biochem. Biophys. Res. Commun. 42*, 705–713.

Que, L., Jr., Anglin, J. R., Bobrik, M. A., Davison, A., & Holm, R. H. (1974) *J. Am. Chem. Soc. 96*, 6042–6048.

Reynolds, J. G., Laskowski, E. J., & Holm, R. H. (1978) *J. Am. Chem. Soc. 100*, 5315–5322.

Sheridan, R. P., Allen, L. C., & Carter, C. W., Jr. (1981) *J. Biol. Chem. 256*, 5052–5057.

Toi, H., La Mar, G. N., Margalit, R., Che, C.-M., & Gray, H. B. (1984) *J. Am. Chem. Soc. 106*, 6213–6217.